nature genetics

© 2005 Nature Publishing Group http://www.nature.com/naturegenetics

Temporal dissection of p53 function *in vitro* and *in vivo*

Maria A Christophorou[1,4], Dionisio Martin-Zanca[1,2,4], Laura Soucek[1], Elizabeth R Lawlor[1,3], Lamorna Brown-Swigart[1], Emmy W Verschuren[1,3] & Gerard I Evan[1]

To investigate the functions of the p53 tumor suppressor, we created a new knock-in gene replacement mouse model in which the endogenous *Trp53* gene is substituted by one encoding p53ER^{TAM}, a p53 fusion protein whose function is completely dependent on ectopic provision of 4-hydroxytamoxifen. We show here that both tissues *in vivo* and cells *in vitro* derived from such mice can be rapidly toggled between wild-type and p53 knockout states. Using this rapid perturbation model, we define the kinetics, dependence, persistence and reversibility of p53-mediated responses to DNA damage in tissues *in vivo* and to activation of the Ras oncoprotein and stress *in vitro*. This is the first example to our knowledge of a new class of genetic model that allows the specific, rapid and reversible perturbation of the function of a single endogenous gene *in vivo*.

The very high frequency with which the p53 pathway is inactivated in human cancers attests to the crucial and pervasive role of p53 as a tumor suppressor. p53 differs from most other characterized tumor suppressors in that it seems to have no substantial role in the checkpoint management of proliferation in normal, unstressed cells[1] but to have evolved specifically to integrate responses to stress and pathological stimuli. Consistent with this idea, p53-deficient mice are generally developmentally normal yet extremely prone to a variety of tumors, principally lymphomas and sarcomas[2].

p53 exerts a highly protean influence on diverse biological processes, making it difficult to define the precise mechanisms by which p53 suppresses neoplasia in any specific instance. Often, inactivation of p53 appears quite late during tumor evolution, suggesting that it has a role in suppressing delayed aspects of tumor progression such as angiogenesis, invasion and genome instability. On the other hand, p53 mediates induction of apoptosis and growth arrest in response to DNA damage and oncogene activation, events required to drive the earliest stages of tumor evolution. Our limited knowledge of how p53 suppresses tumorigenesis in tissues *in vivo* makes it impossible to determine whether absence of p53 function is crucial only at specific, transient stages of tumor evolution, such as when cells sustain acute genotoxic injury or a genome-destabilizing crisis, or whether tumor cells carry persistent p53-activating signals that necessitate sustained loss of p53 function throughout a tumor's natural history. Establishing which of these ideas is true has profound implications for the therapeutic utility of p53 restoration in cancer, as only cancer cells carrying persistent p53-activating signals would be susceptible to the tumor-suppressive influence of restored p53 function.

p53-deficient mice have proven invaluable in the study of p53 function *in vivo* and in determining the consequences of its absence for tumor development. One limitation of constitutive knockout models is that they do not allow for subsequent reversal of p53 status, a prerequisite for understanding the temporal relationship between genotoxic injury and tumor evolution and the role of p53 in mediating the DNA damage response and suppressing cancers. For this reason, we constructed a new knock-in mouse in which endogenous *Trp53* is modified to express an ectopically regulatable form of the p53 protein, p53ER^{TAM}. These mice can be rapidly, reversibly and repeatedly toggled between wild-type and p53-deficient states, allowing direct examination of the temporal requirements for p53 function in response to DNA damage or oncogenic stress in tissues *in vivo* and in cells derived from such mice *in vitro*.

RESULTS

The DNA damage response requires 4-hydroxytamoxifen

We generated mice homozygous with respect to knock-in alleles encoding p53ER^{TAM} (*Trp53*$^{KI/KI}$) by inserting the hormone-binding domain of the modified estrogen receptor, ER^{TAM} (ref. 3), in-frame at the 3′-end of the coding sequence of endogenous *Trp53* (**Fig. 1**). In the absence of 4-hydroxytamoxifen, *Trp53*$^{KI/KI}$ mice developed various forms of tumors. Most were lymphoid in nature, mainly malignant and metastatic thymic lymphomas with characteristic areas of necrosis and macrophage infiltration. The spontaneous incidence and tumor spectrum are similar, albeit slightly delayed, to those seen in classical p53-deficient mice of the same mixed C57BL/6 × 129/SvJ genetic background as our *Trp53*$^{KI/KI}$ mice[2,4,5] (**Fig. 1d**). These

[1]Cancer Research Institute, University of California San Francisco Comprehensive Cancer Center, San Francisco, California 94143-0875, USA. [2]Instituto de Microbiologia Bioquimica CSIC/Universidad de Salamanca, Campus "Miguel de Unamuno," 37007 Salamanca, Spain. [3]Present addresses: University of Southern California Keck School of Medicine, Division of Hematology/Oncology, Children's Hospital of Los Angeles, 4650 Sunset Blvd, Los Angeles, California 90027, USA (E.R.L.); Stanford University, Pathology Department, 300 Pasteur Drive, MC 5324, Stanford, California 94305, USA (E.W.V.). [4]These authors contributed equally to this work. Correspondence should be addressed to G.I.E. (gevan@cc.ucsf.edu).

Published online 29 May 2005; doi:10.1038/ng1572

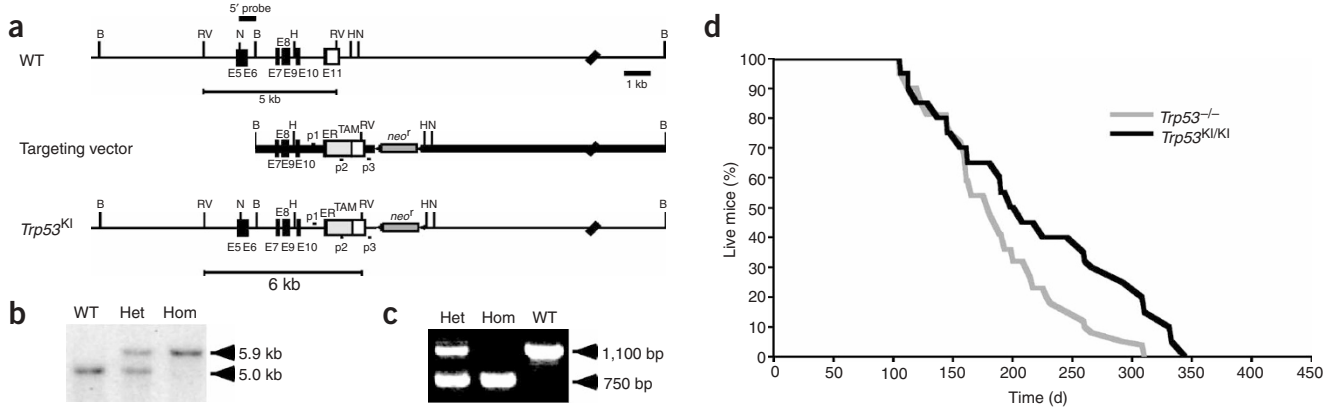

Figure 1 Generation of the *Trp53*^{KI} allele and genotype analysis of *Trp53*$^{KI/KI}$ mice. (**a**) Schematic representation of the 3′ end of the mouse *Trp53* locus, the targeting vector and the *Trp53*^{KI} allele. *Trp53* exons E5 to E11 are shown with coding sequences in black and the untranslated sequences in white. The modified ligand-binding domain of the estrogen receptor is represented by the light gray box (ER^{TAM}), and the *neo* cassette, flanked by *lox*P sites (black arrowheads), as the dark gray box (*neo*^{r}). Also indicated is the external probe (5′ probe) used to genotype the ES cell lines and mice. The 5.0-kb and 6.0-kb bars represent *Eco*RV DNA fragments specific for the wild-type and *Trp53*^{KI} alleles, respectively, which hybridize with the 5′ probe. Relevant restriction sites are shown: B, *Bam*HI; RV, *Eco*RV; N, *Nco*I; H, *Hin*dIII. (**b**) Southern-blot analysis of *Eco*RV-digested genomic DNA from wild-type mice (WT), *Trp53*$^{+/KI}$ mice (Het) and *Trp53*$^{KI/KI}$ mice (Hom), hybridized with the external 5′ probe. Wild-type DNA yields a 5.0-kb fragment, *Trp53*$^{KI/KI}$ DNA yields a 5.9-kb fragment and *Trp53*$^{+/KI}$ DNA yields both fragments. (**c**) Triplex PCR analysis of mouse genomic DNA from wild-type mice (WT), *Trp53*$^{+/KI}$ mice (Het) and *Trp53*$^{KI/KI}$ mice (Hom), using primers p1, p2 and p3. This amplification yields a single 1,100-bp fragment when wild-type DNA is used as template, a single 750-bp fragment with DNA from *Trp53*$^{KI/KI}$ mice and both fragments with DNA from *Trp53*$^{+/KI}$ mice. (**d**) Comparative survival curves for *Trp53*$^{KI/KI}$ ($n = 21$) and *Trp53*$^{-/-}$ ($n = 25$) mice of similar mixed genetic background.

© 2005 Nature Publishing Group http://www.nature.com/naturegenetics

data indicate that, in the absence of activating ligand, p53ER^{TAM} has negligible activity as a tumor suppressor in tumor-prone somatic tissues.

p53 has a crucial role in mediating pathological responses to genotoxic insults, such as γ-irradiation, by triggering growth arrest or apoptosis in radiosensitive tissues such as intestinal epithelium, spleen, bone marrow, thymus, tongue, testis and hair follicles[6–13]. To assess the dependence of such acute genotoxic responses in *Trp53*$^{KI/KI}$ mice on 4-hydroxytamoxifen, we treated 6-week-old mice with systemic 4-hydroxytamoxifen over 48 h to establish wild-type p53 status. We treated control mice with equivalent doses of peanut oil carrier alone. We then exposed mice to 5 Gy of whole body γ-radiation. We collected radiosensitive tissues (spleen, thymus and small intestinal epithelium) after 5 h, identified apoptotic cells in histological sections using the TUNEL assay (**Fig. 2a**) and quantified them (**Fig. 2b**). In *Trp53*$^{KI/KI}$ mice pretreated with 4-hydroxytamoxifen, γ-irradiation induced rapid and extensive apoptosis, similar to that seen in *Trp53*$^{+/+}$ mice (**Fig. 2a**,**b**). In contrast, *Trp53*$^{KI/KI}$ mice treated with oil alone resembled *Trp53*$^{-/-}$ mice, with little radiation-induced apoptosis (**Fig. 2a**,**b**).

To quantify further the extent of radiation-induced apoptosis, we treated *Trp53*$^{+/+}$, *Trp53*$^{+/KI}$ and *Trp53*$^{KI/KI}$ mice with 4-hydroxytamoxifen. We then isolated thymocytes, irradiated them *in vitro* with 3 Gy of γ-irradiation and assayed their viability after various times by flow cytometry. We isolated control thymocytes from mice treated with oil alone. As expected, *Trp53*$^{+/+}$ thymocytes showed a substantial loss of viability after irradiation, which was unaffected by 4-hydroxytamoxifen treatment (**Fig. 2c**). In contrast, *Trp53*$^{KI/KI}$ thymocytes showed radiation-induced death only when isolated from mice exposed to 4-hydroxytamoxifen (**Fig. 2c**). Thymocytes from *Trp53*$^{+/KI}$ mice had the same 4-hydroxytamoxifen–independent radiosensitivity as wild-type cells (**Fig. 2c**), indicating that p53ER^{TAM}, in the absence of 4-hydroxytamoxifen, has no dominant interfering effect over wild-type p53.

To validate further the ability of p53ER^{TAM} to recapitulate wild-type p53 functions when provided with 4-hydroxytamoxifen ligand, we examined its ability to induce *Trp53* transcriptional target genes *in vivo* and *in vitro*. After genotoxic injury, p53 mediates the induction of multiple genes involved in growth arrest and apoptosis (*e.g.*, *Cdkn1a* and *Bbc3*, respectively). We therefore assayed the requirement for 4-hydroxytamoxifen in induction of *Cdkn1a* (also called *p21*^{cip1}) and *Bbc3* (also called *puma*) after DNA damage. p53 was functionally restored in *Trp53*$^{KI/KI}$ mice, which were then exposed to 5 Gy of whole body γ-irradiation. Five hours after irradiation, we collected thymi and used real-time quantitative PCR (Taqman) analysis on total thymus RNA to assess expression of *Cdkn1a* and *Bbc3* relative to controls. Both genes were induced in response to γ-irradiation only in *Trp53*$^{KI/KI}$ mice treated with 4-hydroxytamoxifen (**Fig. 3a**).

Next, we assayed the ability of p53ER^{TAM} to act as a transcriptional regulator of p53 target genes *in vitro*. We cultured early passage (passage 3) mouse embryonic fibroblasts (MEFs) isolated from *Trp53*$^{KI/KI}$ embryos in either the presence or the absence of 4-hydroxytamoxifen and then exposed them to doxorubicin, a well-characterized activator of p53 in MEFs[14]. We then assayed expression of the protein products of the p53 target genes *Cdkn1a* and *Mdm2* in each MEF population by immunoblot analysis. We used *Trp53*$^{+/+}$ and *Trp53*$^{-/-}$ MEFs as controls. In the presence of 4-hydroxytamoxifen, doxorubicin induced expression of p21^{cip1} and Mdm-2 in *Trp53*$^{KI/KI}$ MEFs to levels comparable with those in *Trp53*$^{+/+}$ cells (**Fig. 3b**). In the absence of 4-hydroxytamoxifen, induction of those proteins was greatly reduced; Mdm-2 was expressed at a level similar to that seen in *Trp53*$^{-/-}$ MEFs. Although the amount of p21^{cip1} was modestly elevated relative to that in *Trp53*$^{-/-}$ MEFs, perhaps reflecting some residual low-level p53 activity in the absence of 4-hydroxytamoxifen, it was insufficient to exert any inhibitory effect on cell cycle progression.

ER^{TAM} fusion proteins are reversibly switchable because they require the continuous presence of 4-hydroxytamoxifen ligand for function. To establish the kinetics of functional deactivation of

© 2005 Nature Publishing Group http://www.nature.com/naturegenetics

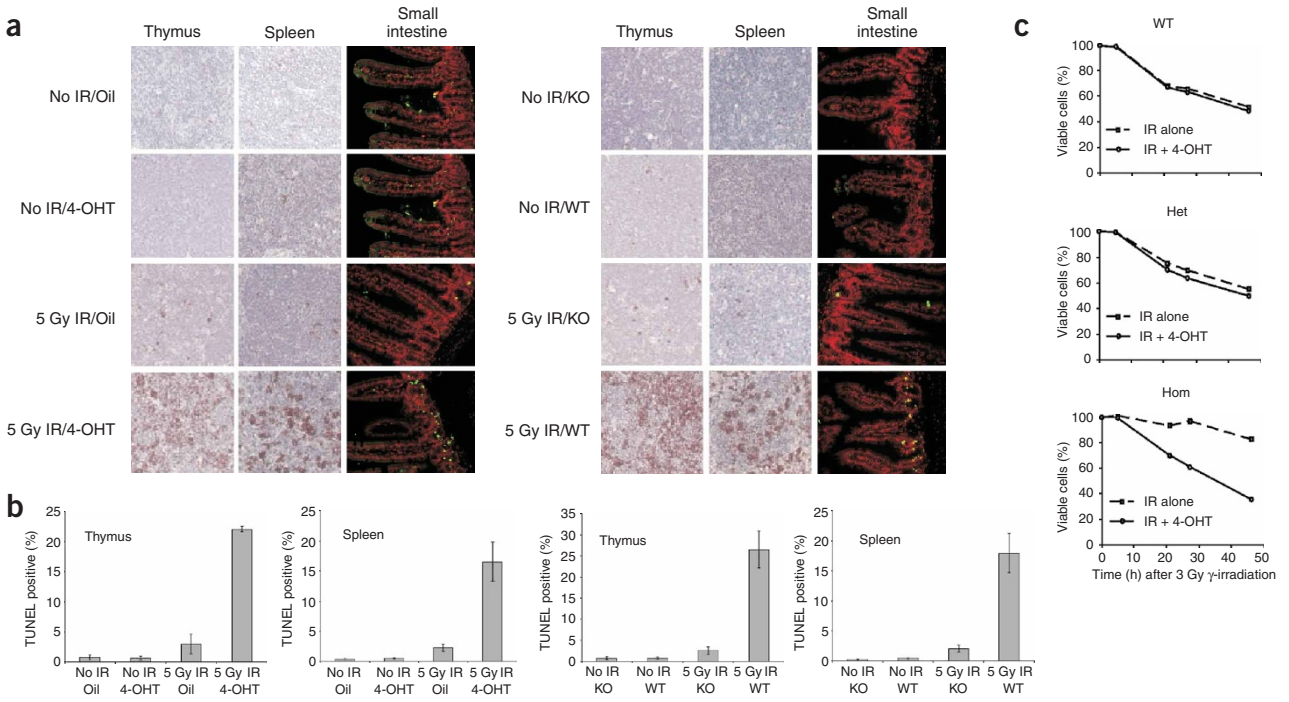

Figure 2 4-Hydroxytamoxifen (4-OHT) restores the p53-mediated damage response in *Trp53*$^{KI/KI}$ mouse tissues *in vivo* and cells *in vitro*. (**a**) TUNEL apoptosis staining on paraffin sections of thymus, spleen and small intestine from wild-type (WT), *Trp53*$^{-/-}$ (KO; right) and *Trp53*$^{KI/KI}$ mice (left). For thymus and spleen, peroxidase TUNEL staining is brown and hematoxylin nuclear counterstain is blue. For small intestine, fluorescein TUNEL staining is green and propidium iodide nuclear counterstain is red. γ-radiation–induced apoptosis is confined to the crypts of the small intestinal epithelium. (**b**) Apoptosis for spleen and thymus was quantified by counting three representative fields of 500 cells from each of three samples of mouse thymus and spleen. (**c**) Propidium iodide exclusion and flow cytometry apoptotic assays of thymocytes from wild-type (WT), *Trp53*$^{+/KI}$ (Het) and *Trp53*$^{KI/KI}$ (Hom) mice. All data points were normalized to unirradiated control thymocytes from the same mice (80% of the untreated cells were viable 24 h after the start of the experiment, and 25% at 48 h).

p53ER^{TAM} after surcease of 4-hydroxytamoxifen *in vivo*, we treated 6-week-old *Trp53*$^{KI/KI}$ mice with two daily intraperitoneal injections of 4-hydroxytamoxifen and then exposed them to 2.5 Gy of γ-irradiation at various times after the final injection. Five hours after irradiation, we isolated radiosensitive tissues and assessed and quantified histochemically the TUNEL-positive apoptotic cells. We included unirradiated mice as controls. We observed substantial apoptosis when p53 function was restored within 2 h of irradiation, but this rapidly attenuated after withdrawal of 4-hydroxytamoxifen. In the thymus (**Fig. 4a,b**) and spleen (**Fig. 4c,d**), the apoptotic response was largely lost by 48–72 h after 4-hydroxytamoxifen withdrawal and completely vanished by 120 h. Loss of the apoptotic response was even more rapid in the small intestine (**Fig. 4e,f**), perhaps owing to the rapid turnover of cells in this tissue.

These data demonstrate the continuous dependency for 4-hydroxytamoxifen of p53-dependent transcriptional and biological responses to DNA damage in tissues *in vivo* and cells *in vitro* from *Trp53*$^{KI/KI}$ mice.

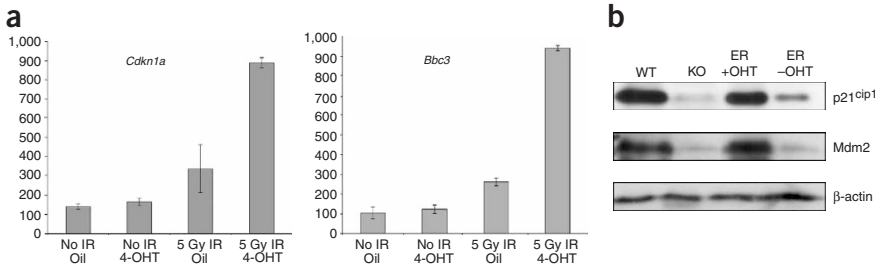

Figure 3 4-Hydroxytamoxifen (4-OHT) restores the p53-mediated transcriptional regulation in *Trp53*$^{KI/KI}$ mouse tissues *in vivo* and cells *in vitro*. (**a**) Taqman analysis of p53 transcriptional target genes on total RNA isolated from whole thymus of *Trp53*$^{KI/KI}$ mice. All data points were created by triplicate reactions and from three individual mice. RNA levels relative to β-glucuronidase are shown. (**b**) Immunoblot analysis of p53 transcriptional targets, using whole-cell lysates from early-passage wild-type (WT), *Trp53*$^{-/-}$ (KO) and *Trp53*$^{KI/KI}$ MEFs that were cultured in either the presence (ER+OHT) or the absence (ER–OHT) of 4-hydroxytamoxifen. β-actin shows equal loading.

4-Hydroxytamoxifen renders p53ER^{TAM} competent to be activated

A prerequisite for use of the *Trp53*$^{KI/KI}$ mouse model is that 4-hydroxytamoxifen should not activate p53ER^{TAM} on its own but rather render it competent for activation in response to appropriate upstream signals. To confirm that this was the case, we treated *Trp53*$^{KI/KI}$ mice systemically with 4-hydroxytamoxifen for various lengths of time in the absence of any overt genotoxic insult. We then isolated various tissues and examined them for any 4-hydroxytamoxifen–dependent changes in architecture (hematoxylin and eosin staining; data not shown) and apoptosis (TUNEL staining; **Fig. 2a,b**). Analysis of liver, lung, small intestine, heart, kidney, spleen, thymus

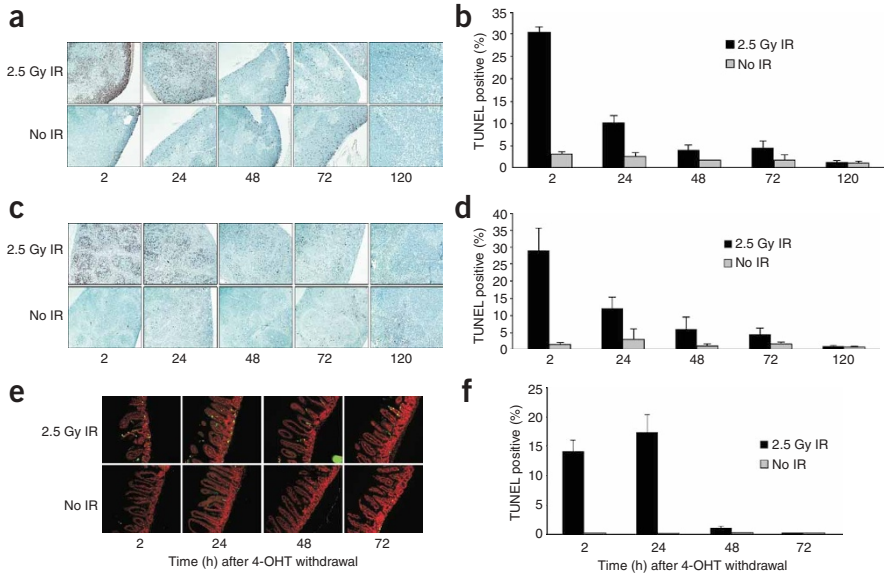

Figure 4 The *Trp53*$^{KI/KI}$ system is competent for deactivation of p53ER^{TAM}. (**a**,**c**,**e**) TUNEL staining of apoptotic cells in paraffin-embedded sections of thymus (**a**), spleen (**c**) and small intestine (**e**) derived from *Trp53*$^{KI/KI}$ mice. Times shown represent the time of irradiation after the final 4-hydroxytamoxifen (4-OHT) injection. For thymus and spleen, peroxidase TUNEL staining is brown and hematoxylin nuclear counterstain is blue. For small intestine, fluorescein TUNEL staining is green and propidium iodide DNA counterstain is red. γ-radiation–induced apoptosis is confined to the crypts of the small intestinal epithelium. Tissue sections from nonirradiated controls are shown in the bottom panels. Some nonspecific stromal fluorescein stain can be seen in the intestine. (**b**,**d**,**f**) Apoptosis in the above samples was quantified by counting three representative fields of 500 cells from each of three samples of mouse thymus (**b**), spleen (**d**) and intestine (**f**).

and epidermis from *Trp53*$^{KI/KI}$ mice showed no evidence of tissue pathology or induction of apoptosis due to 4-hydroxytamoxifen (data not shown; **Fig. 3a**). Furthermore, extended (up to 30 days) treatment of 'unstressed' *Trp53*$^{KI/KI}$ mice with 4-hydroxytamoxifen had no measurable impact on viability, well-being or tissue architecture (data not shown).

p53-activating signals induced by DNA damage are short-lived

Although it is well established that p53 is a crucial mediator of the rapid response to acute DNA damage observed in many tissues[15], it is not certain how long such damage, or the p53-activating signals it triggers, persists in different tissues *in vivo*. Because p53 competence is so rapidly restored in tissues after systemic administration of 4-hydroxytamoxifen to *Trp53*$^{KI/KI}$ mice, we were able to assess the persistence of the damage-induced p53-activating signals in different tissues *in vivo* by inducing acute DNA damage and then restoring p53 function at various times thereafter.

We exposed *Trp53*$^{KI/KI}$ mice to a single dose of 2.5 Gy of γ-irradiation and then functionally restored p53 by systemic administration of 4-hydroxytamoxifen 6, 24, 48, 72 and 96 h later. Abundant apoptosis is evident by 5 h after irradiation in radiosensitive tissues of *Trp53*$^{+/+}$ mice[16], and so we monitored cell death in *Trp53*$^{KI/KI}$ tissues 5 h after p53 restoration. The p53 response to radiation persisted for only a relatively short time after the insult, although the kinetics of persistence varied somewhat among tissues (**Fig. 5**). The p53-dependent apoptotic response to DNA damage was undetectable above background by 72 h after the insult in thymus (**Fig. 5a**,**b**) and spleen (**Fig. 5c**,**d**) and by 96 h after the insult in small intestine (**Fig. 5e**,**f**). Therefore, p53-activating signals initiated by acute radiation injury decay rapidly in radiosensitive tissues *in vivo*.

Reversible regulation of p53 status in *Trp53*$^{KI/KI}$ MEFs *in vitro*

We next used primary MEFs derived from *Trp53*$^{KI/KI}$ mice to explore *in vitro* the temporal requirements for p53 function in

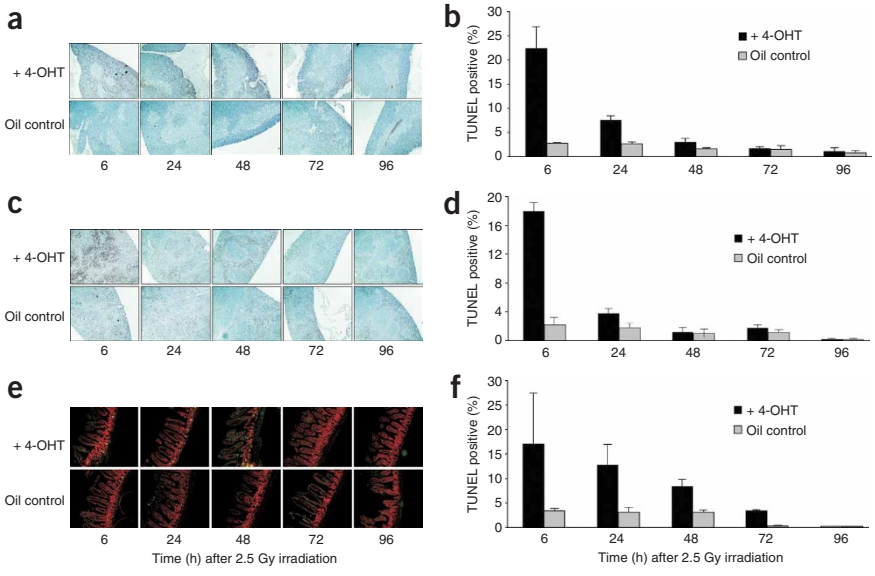

Figure 5 Persistence of DNA damage–induced p53 activating signal. (**a**,**c**,**e**) TUNEL staining of apoptosis in paraffin-embedded sections of thymus (**a**), spleen (**c**) and small intestine (**e**) from *Trp53*$^{KI/KI}$ mice. Times shown represent the time of 4-hydroxytamoxifen (4-OHT) injection after a single irradiation insult. For thymus and spleen, peroxidase TUNEL staining is brown and hematoxylin nuclear counterstain is blue. For small intestine, fluorescein TUNEL staining is green and propidium iodide DNA counterstain is red. γ-radiation–induced apoptosis is confined to the crypts of the small intestinal epithelium. Tissue sections from oil-injected controls are shown in the bottom panels. Some nonspecific stromal fluorescein stain can be seen in the intestine. (**b**,**d**,**f**) Apoptosis in the above samples was quantified by counting three representative fields of 500 cells from each of three samples of mouse thymus (**b**), spleen (**d**) and intestine (**f**).

© 2005 Nature Publishing Group http://www.nature.com/naturegenetics

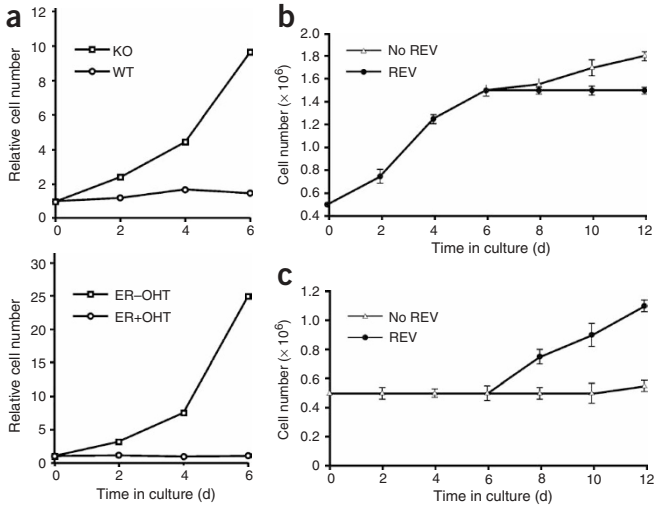

Figure 6 Response to Ras deregulation is dependent on 4-hydroxytamoxifen (4-OHT) and reversible. (**a**) Growth curves of MEFs expressing activated H-Ras V12. Wild-type, *Trp53*$^{-/-}$ (KO) and *Trp53*$^{KI/KI}$ MEFs that were cultured either in the presence (ER+OHT) or absence (ER–OHT) of 100 nM 4-hydroxytamoxifen. Cells were counted and placed in culture after 48 h of puromycin selection (day 0) and then counted every 2 d thereafter. (**b**) *Trp53*$^{KI/KI}$ MEFs expressing Ras V12 were propagated in the absence of 4-hydroxytamoxifen for 6 d. At day 6, the culture was split; half the cells were seeded in medium without 4-hydroxytamoxifen (no REV), and the other half was exposed to 100 nM 4-hydroxytamoxifen to restore p53 function (REV). Cell numbers were then determined in each culture every 2 d. (**c**) *Trp53*$^{KI/KI}$ MEFs expressing Ras V12 were propagated in culture in the presence of 100 nM 4-hydroxytamoxifen for 6 d. At day 6, the culture was split; half the cells were seeded in medium containing 100 nM of 4-hydroxytamoxifen (no REV), and the other half was seeded in 4-hydroxytamoxifen–free medium (REV). Cell numbers were then determined in each culture every 2 d.

© 2005 Nature Publishing Group http://www.nature.com/naturegenetics

mediating responses to deregulated oncogenes and DNA damage. One well characterized example of p53 antagonizing oncogene activation is the potent induction of growth arrest or replicative senescence by activated Ras in cultured MEFs[17]. To explore the dependency on 4-hydroxytamoxifen of this phenomenon in *Trp53*$^{KI/KI}$ MEFs, we infected early-passage cells with an H-Ras V12 retroviral vector and monitored their proliferation in the presence or absence of 4-hydroxytamoxifen. In the presence of 4-hydroxytamoxifen, expression of activated H-Ras triggered growth arrest in *Trp53*$^{KI/KI}$ MEFs (**Fig. 6a**), accompanied by expression of senescence-associated (SA)-β-galactosidase and progressive emergence of cells with classic hallmarks of senescence, such as gross enlargement and vacuolization (data not shown). In contrast, H-Ras–expressing *Trp53*$^{KI/KI}$ MEFs cultured without 4-hydroxytamoxifen continued to proliferate, did not express measurable SA-β-galactosidase and showed no signs of premature senescence. This phenotype mimics the respective behaviors of wild-type and *Trp53*$^{-/-}$ MEFs expressing deregulated H-Ras (**Fig. 6a**).

Ras is thought to trigger p53-dependent growth arrest through induction of the ARF tumor suppressor[18]. It is not known, however, whether such p53-dependent growth arrest is an acute response to the transition from normal to activated Ras or whether oncogenic Ras transduces a persistent p53-activating signal. To address this issue, we expressed activated H-Ras in *Trp53*$^{KI/KI}$ MEFs in the absence of 4-hydroxytamoxifen and allowed the cells to grow in a p53-null state for several passages. Subsequent restoration of p53 function triggered immediate cell cycle arrest, unambiguously showing that activated Ras elicits a persistent p53-triggering signal in cells (**Fig. 6b**).

To explore whether p53 function is required to maintain Ras-induced growth arrest, we exposed *Trp53*$^{KI/KI}$ MEFs expressing activated H-Ras to 4-hydroxytamoxifen for 6 d, at which time all measurable proliferation had ceased and many cells were phenotypically senescent. We then removed 4-hydroxytamoxifen to deactivate p53 function, after which most cells reentered the cell cycle (**Fig. 6c**) and, thereafter, propagated indefinitely. Thus, at least in most cells, p53 function is required to maintain Ras-induced growth

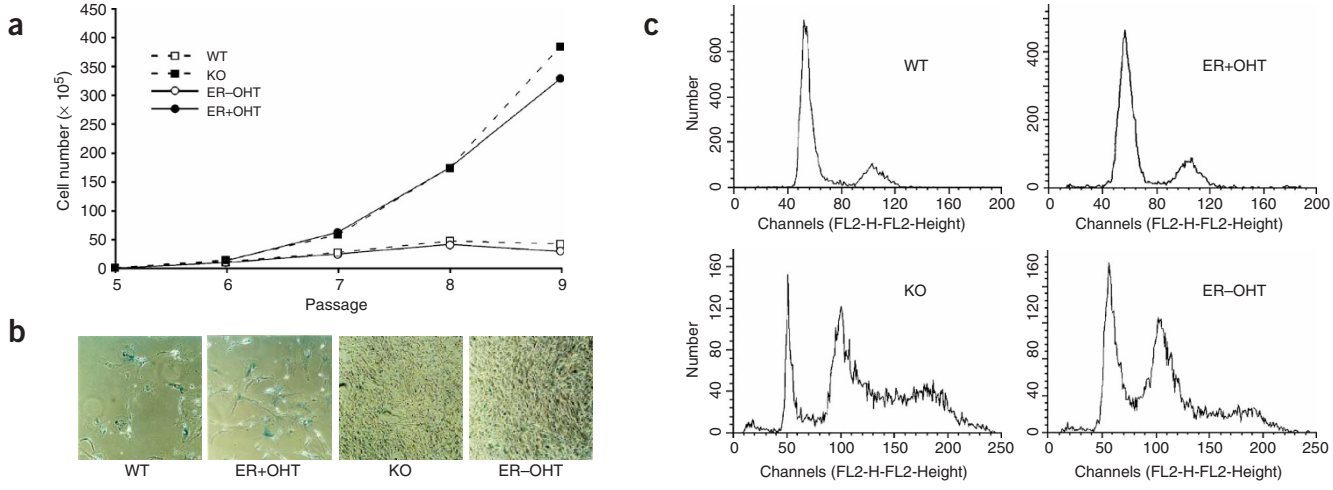

Figure 7 4-Hydroxytamoxifen (4-OHT) determines the immortalization, senescence and ploidy states of primary p53ER^{TAM} cells. (**a**) Growth curves of MEFs from wild-type (WT), *Trp53*$^{-/-}$ (KO) and *Trp53*$^{KI/KI}$ MEFs treated with 100 nM 4-hydroxytamoxifen (ER+OHT) or ethanol control (ER–OHT). (**b**) SA-β-galactosidase staining of the same cell types at passage 12. Pictures are taken at ×10 magnification. (**c**) Cell cycle profiles of the same cell populations at passage 12, obtained by flow cytometric analysis of propidium iodide incorporation by fixed cells.

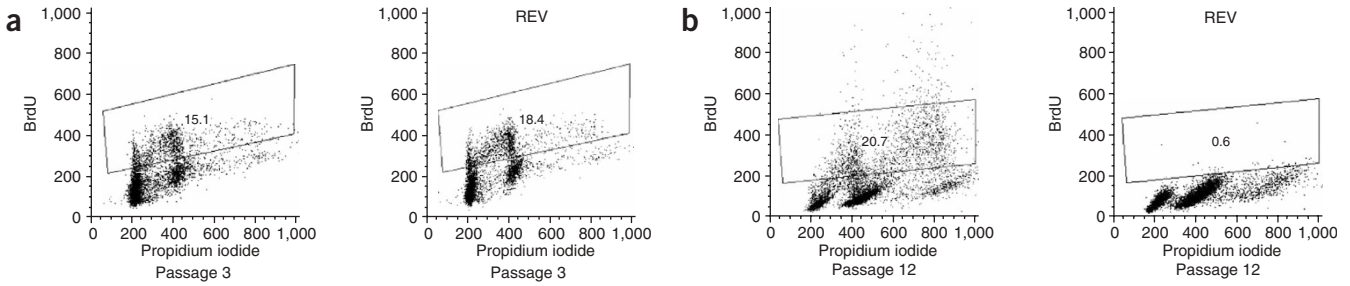

Figure 8 Late-passage, but not early-passage, cultured primary fibroblasts activate p53 in the absence of any overt DNA damage or stress. (**a**,**b**) BrdU–propidium iodide flow cytometric analysis of passage 3 (**a**) and passage 12 (**b**) *Trp53*$^{KI/KI}$ MEFs. Cells were propagated in culture in the absence of 4-hydroxytamoxifen up to passage 2 (**a**) or passage 11 (**b**), and then 100 nM of 4-hydroxytamoxifen was added to the medium for one passage (3 d; REV samples, right). Propidium iodide incorporation is represented on the *x* axis. BrdU incorporation is represented on the *y* axis. (**c**) Immunoblot analysis of p21^{cip1} expression in whole-cell lysates derived from the above cell populations at passages 3 and 12. β-actin shows equal loading.

arrest. But not all Ras-arrested cells reentered the cell cycle upon p53 deactivation. The 6-day-old cultures of Ras-arrested MEFs were highly heterogeneous with respect to the extent of phenotypic senescence. Detailed videomicroscopic analysis showed that the largest and most vacuolated Ras-arrested MEFs did not reenter the cell cycle and remained positive for β-galactosidase upon p53 de-activation (data not shown). These irreversibly senescent cells were rapidly diluted by proliferating cells as the cultures were propagated.

MEFs acquire p53-activating signals while cultured *in vitro*

After approximately eight or nine passages *in vitro*, primary MEFs undergo proliferative arrest thought to be induced by the ill-defined stress of growth in cultured[19]. The arrest is p53-dependent, occurs in both G1 and G2 and is characterized by expression of SA-β-galactosidase and a senescent phenotype. By contrast, *Trp53*$^{-/-}$ MEFs do not arrest, express SA-β-galactosidase or senesce, and by approximately passage 12 most cells in *Trp53*$^{-/-}$ MEF cultures show aberrations in chromosomal number. These immortalized cells can be propagated indefinitely.

To compare the behavior of *Trp53*$^{KI/KI}$ MEFs with and without 4-hydroxytamoxifen with that of wild-type and *Trp53*$^{-/-}$ MEFs, we explanted *Trp53*$^{KI/KI}$ MEFs into culture medium in either the presence or the absence of 4-hydroxytamoxifen and propagated them. *Trp53*$^{KI/KI}$ MEFs grown *in vitro* in the presence of 4-hydroxytamoxifen resembled wild-type MEFs, undergoing growth arrest within a few passages (**Fig. 7a**). The arrested cells expressed SA-β-galactosidase and appeared morphologically senescent (**Fig. 7b**). In contrast, *Trp53*$^{KI/KI}$ MEFs cultured in the absence of 4-hydroxytamoxifen behaved exactly like *Trp53*$^{-/-}$ MEFs, expanding progressively without crisis or expression of SA-β-galactosidase (**Fig. 7a**,**b**). To assess the impact of p53 functional status on genome integrity, we analyzed the DNA content of MEFs propagated for 12 passages by flow cytometry. DNA content of both wild-type MEFs and *Trp53*$^{KI/KI}$ MEFs cultured in the presence of 4-hydroxytamoxifen was confined to 2N and 4N G1 and G2 populations, with no cells in S phase or with >4N DNA content (**Fig. 7c**). In contrast, *Trp53*$^{-/-}$ MEFs and *Trp53*$^{KI/KI}$ MEFs cultured in the absence of 4-hydroxytamoxifen had substantial S-phase, aneuploid and polyploid populations (**Fig. 7c**). Thus, *Trp53*$^{KI/KI}$ MEFs recapitulate wild-type and *Trp53*$^{-/-}$ phenotypes *in vitro*, depending on availability of 4-hydroxytamoxifen.

To determine whether there might be a relationship between aberrant chromosome complement and responses of cultured MEFs to p53 restoration, we examined the consequences of restoring p53 function to early-passage (passage 3) *Trp53*$^{KI/KI}$ MEFs, which have ostensibly normal diploid chromosome content, and to late-passage (passage 12) MEFs, which have largely aberrant chromosome content. We cultured explanted *Trp53*$^{KI/KI}$ MEFs in the absence of 4-hydroxytamoxifen for either 3 or 12 passages *in vitro* and then restored p53 function by adding 4-hydroxytamoxifen. We then monitored cell proliferation and induction of p21^{cip1}. Passage 3 cells were unaffected by restoration of functional p53 (**Fig. 8a**), had only marginal p21^{cip1} induction (**Fig. 8c**) and continued to proliferate like wild-type MEFs until arresting around passages 6–8 (data not shown). In contrast, p53 restoration in passage 12 MEFs triggered immediate growth arrest with loss of S-phase population (**Fig. 8b**). The arrest was accompanied by strong upregulation of p21^{cip1} (**Fig. 8c**). Thus, although passage 3 and passage 12 cells are both ostensibly exposed to the same incident *in vitro* stresses, only late-passage cells carry constitutive signals that engage p53 upon its restoration.

DISCUSSION

The inactivation of p53 or its attendant pathway in human cancer is evidence of its role as a tumor suppressor. The diversity of signals that activate p53, including DNA damage, hypoxia, nutrient privation and oncogene activation, and the diversity of biological outcomes that such activation can elicit (cell death, transient or permanent growth arrest, DNA repair and suppression of invasion and angiogenesis) have made it difficult to define when, where and why p53 acts to suppress cancer. In particular, it is not known whether the signals that activate p53 during tumor evolution are episodic or persistent and, consequently, what might be the consequence of restoring p53 function in an established tumor.

To define directly the role of p53 in different tissues and at different stages of tumor evolution, we constructed a switchable knock-in mouse model in which endogenous p53 can be reversibly switched between functional and nonfunctional states by modifying endogenous *Trp53* to encode the 4-hydroxytamoxifen–dependent p53ER^{TAM} protein[3]. Expression of p53ER^{TAM} is controlled by the same orthotopic transcriptional regulatory sequences that normally regulate *Trp53* expression in each tissue *in vivo*, but the expressed p53ER^{TAM} protein is functionally competent only in the presence of

© 2005 Nature Publishing Group http://www.nature.com/naturegenetics

© 2005 Nature Publishing Group http://www.nature.com/naturegenetics

4-hydroxytamoxifen ligand. This *Trp53*$^{KI/KI}$ mouse model provides a platform for highly specific and temporally controlled perturbation analysis of p53 function both in mouse tissues *in vivo* and in explanted primary cells derived from such tissues *in vitro*.

As expected, *Trp53*$^{KI/KI}$ mice in the absence of 4-hydroxytamoxifen had a high incidence and spectrum of spontaneous lymphoma, similar to isogenic *Trp53*$^{-/-}$ mice. In addition, radiosensitive tissues in *Trp53*$^{KI/KI}$ mice not exposed to 4-hydroxytamoxifen, such as thymus, spleen and intestinal epithelium, were refractory to radiation-induced apoptosis. But systemic administration of 4-hydroxytamoxifen to *Trp53*$^{KI/KI}$ mice rapidly restored p53 function in tissues, re-establishing radiosensitivity to thymus, spleen and intestinal epithelium in as little as 2 h after intraperitoneal administration of 4-hydroxytamoxifen (data not shown). Similarly, p53 competence was also restored rapidly in thymocytes and MEFs *in vitro* after addition of 4-hydroxytamoxifen to the culture medium. Subsequent withdrawal of 4-hydroxytamoxifen from mice or cells reverts them to p53-deficient status, demonstrating the rapid and repeatable reversibility of p53 function in the *Trp53*$^{KI/KI}$ model. Such analyses show that restoration of p53 function by 4-hydroxytamoxifen administration does not, of itself, activate p53ER^{TAM} but rather renders it competent to become activated in response to appropriate upstream damage and stress signals.

Given the proclivity of both normal and neoplastic cells *in vitro* and *in vivo* to undergo rapid genome destabilization in the absence of p53 (refs. 20,21), it seems likely that tissues of *Trp53*$^{KI/KI}$ mice not treated with 4-hydroxytamoxifen would acquire an appreciable load of genetic defects during embryonic development and postnatal life. Nonetheless, restoration of p53 function to unstressed mice led to no measurable p53 activation. As overtly damaged cells would be expected to respond to p53 restoration by triggering activation of p53 target genes and p53-associated pathologies, this indicates that they do not accumulate in p53-deficient mice in substantial numbers. This is consistent with our demonstration that p53 restoration triggers p53-dependent apoptosis only within the first 48–72 h after acute radiation injury, indicating that p53-activating signals induced by DNA damage attenuate very rapidly in somatic cells, most probably because the damage is expeditiously resolved. Thus, although p53 has previously been directly implicated in efficient induction of various components of the nucleotide excision repair and base excision repair machinery[22,23], our data suggest that absence of p53 function does not compromise efficient resolution of radiation-induced genotoxic injury in somatic cells *in vivo*.

There are some suggestions that fusing ER^{TAM} to p53 decreases somewhat the dynamic range of p53 function. For example, we found evidence of low-level basal activity in the absence of 4-hydroxytamoxifen ligand, exemplified by the higher basal level of p21^{cip1} in cultured *Trp53*$^{KI/KI}$ MEFs *in vitro* (**Fig. 3**). Such basal 'leakiness' may be responsible for the slight delay we observed in the incidence of spontaneous tumorigenesis in *Trp53*$^{KI/KI}$ mice never treated with 4-hydroxytamoxifen when compared with isogenic *Trp53*$^{-/-}$ mice (**Fig. 1d**). In addition, we observed a slight decrease in maximal p21^{cip1} levels after addition of 4-hydroxytamoxifen to cultured MEFs, potentially indicating that maximal p53ER^{TAM} activity is less than that of wild-type p53. Consistent with this possibility, Taqman analysis indicated that peak levels of the p53 target genes *Cdkn1a* and *Bbc3* after irradiation were up to two times lower in *Trp53*$^{KI/KI}$ tissues treated with 4-hydroxytamoxifen than in wild-type tissues (data not shown). But this has no measurable impact on any aspect of p53-dependent biology that we can discern, whether it be the response to DNA damage *in vivo* or to activation of oncogenes or culture stress *in vitro*.

For p53 restoration to exert any therapeutic effect in established cancers, tumor cells must carry sustained p53-activating signals that can engage the restored p53. But our data indicate that each instance of DNA damage triggers p53 activation only transiently, suggesting that DNA damage is unlikely to support sustained p53 activation—unless, for example, tumor cells have irresolvable DNA lesions. In contrast to DNA damage, activation of oncogenes is likely to be a persistent feature of tumor cells. Although oncogenes are known to activate p53 by means of the ARF tumor suppressor, however, it is not known whether such activation is sustained or whether there is only a transient response to the abrupt transition from normal to abnormal oncogene activity in the cell. To discriminate between these two possibilities, we established MEFs expressing constitutively activated Ras and proliferating in the absence of functional p53 and then restored p53 competence. We observed the immediate growth arrest and onset of replicative senescence, indicating that activated Ras projects persistent p53-activating signals in these cells. Furthermore, p53 function is required to maintain Ras-induced arrest once established, as subsequent deactivation of p53ER^{TAM} triggers widespread cell cycle entry.

MEFs cultured *in vitro* rapidly undergo p53-dependent replicative senescence at approximately passage 8 (equivalent to ~14–18 population doublings in our 3T9 protocol). This arrest is distinct from classical Hayflick arrest in human fibroblasts associated with telomere erosion[24] and seems to be caused by the cumulative impact of ill-defined *in vitro* stresses ('culture shock')[19]. p53-deficient MEFs have marked genomic instability, principally centrosome amplification and aberrant ploidy. In *Trp53*$^{KI/KI}$ MEFs *in vitro*, both replicative senescence and genomic instability are determined by the presence or absence of p53, allowing us to address questions about the timing, persistence and irreversibility of these p53-dependent phenomena. Notably, restoration of functional p53 to early-passage, diploid *Trp53*$^{KI/KI}$ MEFs induces no detectable growth arrest and elicits only very modest induction of p53 target genes, whereas p53 restoration in late-passage *Trp53*$^{KI/KI}$ MEFs triggers both widespread arrest and potent induction of p53 targets. Thus, although both early- and late-passage MEFs are presumably in receipt of the same incident *in vitro* stresses, only late-passage cells carry p53-activating signals. These observations argue that it is not the incident stress of culture *per se* that triggers p53 activation in MEFs, but rather that the sustained propagation *in vitro* promotes the onset of some catastrophic and irreversible event that, thereafter, propagates a constitutive p53-activating signal. The p53-induced arrest of late-passage cells is essentially irreversible upon p53 deactivation (data not shown), quite unlike that induced by Ras activation, suggesting that activated oncogenes are not the source of such p53-activating signals. One alternative candidate p53 trigger in late-passage MEFs is aberrant ploidy, which is typically linked to aberrant centrosome number, itself a process directly monitored by p53-dependent checkpoints[25].

The data derived from both *in vivo* and *in vitro* studies using our switchable *Trp53*$^{KI/KI}$ model shed new light on p53 biology regarding the timing and persistence of the signals that activate p53 in normal, damaged and neoplastic cells. Our studies define, for the first time to our knowledge, the important kinetic distinction between DNA damage signals, essentially ephemeral in nature, and the persistent p53-activating signals induced by oncogenic lesions and (potentially) aberrant chromosome complement. In the future, the *Trp53*$^{KI/KI}$ model should prove invaluable in determining the relative importance and timing of these diverse signaling modalities during different stages of tumor evolution.

METHODS

Generation of *Trp53*$^{KI/KI}$ mice. We isolated genomic clones encompassing wild-type *Trp53* from ES-129/SvJ cells. We screened a BAC-based genomic

© 2005 Nature Publishing Group http://www.nature.com/naturegenetics

library made from ES-129/SvJ cells (Genome Systems) by PCR using oligonucleotides 106660 and 106663, which were derived from exons 10 and 11 of mouse *Trp53*, respectively. These oligonucleotides amplified an 800-bp DNA fragment encompassing intron 10 of *Trp53*. This strategy allows for the discrimination between clones containing the genomic locus from those containing the *Trp53* pseudogene (which would yield a 215-bp amplification fragment). We isolated three BAC clones and analyzed them by Southern blotting for the presence of an 11-kb *Bam*HI DNA fragment corresponding to the 3′ end of mouse *Trp53* (ref. 26). We subcloned this fragment, which extends from intron 6 to the last exon of *Trp53* and 7 kb downstream, into pBR322 to improve its stability in bacteria. A map of the region is shown in **Figure 1a**.

Generation of the targeting vector. We subcloned a 2.1-kb *Hin*dIII fragment corresponding to the 3′ end of *Trp53*, containing exons 10 and 11, into pSP72 and used it to insert the sequences encoding a modified ligand-binding domain of the mouse estrogen receptor (ER^{TAM}), which binds 4-hydroxytamoxifen but not endogenous estrogens[27]. We fused these sequences, encoding amino acids 281–599 of the receptor, in-frame to the coding sequences of p53, introducing three new amino acids at the junction. The ER^{TAM} sequences are followed by the intact 3′ untranslated sequences of *Trp53*, including its polyadenylation signal. For selection, we introduced a *lox*P-flanked *neo*^{r} cassette 580 bp downstream from the polyadenylation site of *Trp53*. We used the resulting 4.5-kb *Hin*dIII DNA fragment to replace the endogenous 2.1-kb fragment in the context of the 11-kb genomic clone described above. We introduced a unique *Not*I restriction site at the 5′ end of the construct so that it could be linearized before electroporation. The complete targeting vector is represented in **Figure 1a**.

Electroporation of ES cells and selection of homologous recombinant clones. We linearized the targeting vector and introduced it into 129/1 embryonic stem (ES) cells, passage 9, using a Bio-Rad electroporator set at 500 μFd, 240 KV. We selected ES cell clones in Dulbecco's modified Eagle medium supplemented with 15% fetal calf serum, 1,000 units ml^{-1} LIF and 200 mg ml^{-1} G418-containing medium and analyzed them for homologous recombination by Southern blotting. We analyzed DNAs from 204 independent clones by *Eco*RV digestion and hybridization with a probe external to the targeting vector (5′ probe; **Fig. 1a**). This probe hybridizes with a 5-kb DNA fragment in wild-type cells and with an additional 5.9-kb fragment in cells that have undergone homologous recombination (**Fig. 1b**). We further characterized candidate clones using 3′-end and neo-derived probes; we selected five homologous recombinant clones and karyotyped them before using them to generate mouse chimeras.

Chimera generation and breeding. We injected ES clones 2A7 and 2F7 into C57BL/6-derived blastocysts. We backcrossed black/brown chimeric mice to C57BL/6 mice and confirmed germline transmission of the modified $Trp53^{KI}$ allele by Southern-blot analysis. No difference was evident between the two lines, and we used one (2F7) for further study. We intercrossed $Trp53^{+/KI}$ mice to obtain $Trp53^{KI/KI}$ mice. For routine genotyping of the litters, we designed a triplex PCR amplification protocol using oligonucleotides p1 (intron 10.1), p2 (mer550rev) and p3 (106904; **Fig. 1a**). This protocol yields a single 1,100-bp fragment when wild-type DNA is used as template, a single 750-bp fragment with DNA homozygous with respect to the $Trp53^{KI}$ allele, and both fragments with heterozygous DNA (**Fig. 1c**).

Perturbation of p53ER^{TAM} status. The active ligand for ER^{TAM} is 4-hydroxytamoxifen, a metabolite of tamoxifen generated in the liver. 4-Hydroxytamoxifen rapidly equilibrates with all tissues and organs[28]. To restore p53 to wild-type status in $Trp53^{KI/KI}$ mice, we administered 1 mg of tamoxifen dissolved in peanut oil carrier daily by intraperitoneal injection for as long as p53 functionality was required. Control mice were given peanut oil carrier alone. For *in vitro* studies, we included 100 nM of 4-hydroxytamoxifen in 100% ethanol in the culture medium. Equivalent volumes of ethanol alone were used in control cultures.

Cell culture. We isolated primary MEFs from wild-type, $Trp53^{-/-}$ and $Trp53^{KI/KI}$ embryos at embryonic day 13.5 and cultured them in Dulbecco's modified Eagle medium (Invitrogen) supplemented with 10% fetal bovine serum (Invitrogen) and 1% penicillin/G-streptomycin sulfate (Invitrogen). When appropriate, we added 100 nM 4-hydroxytamoxifen (Sigma) in 100% ethanol, or an equal volume of ethanol control, to the medium. The cells were passaged using a standard 3T9 protocol.

Retroviral vectors and gene transfer. We introduced oncogenic H-*ras* (V12) into MEFs using a pLXSP3-V12 Ras vector (a gift from P. Rodrigez-Viciana, University of California San Francisco). We selected infected cell populations in puromycin (2.5 μg ml^{-1} for 3 d) and kept them in puromycin-containing medium thereafter.

p53 target gene analysis: protein isolation. We washed cells once with phosphate-buffered saline and lysed them *in situ* in SDS lysis buffer (2.5% SDS, 0.25 M Tris (pH 6.8) in water). We collected cell lysates with a cell scraper, boiled them at 100 °C for 2 min, passed them several times through a 21-gauge needle and centrifuged them to shear and then pellet chromosomal DNA. We determined the total protein concentration of each supernatant using the Bio-Rad D_C Protein Assay system.

Immunoblot analysis. We fractionated cell lysates (40 μg of total protein) by SDS-PAGE and transferred them for 1 h at 200 mA to nitrocellulose membrane (Immobilon, Millipore) using a wet transfer apparatus. We blocked Immobilon membranes for 1 h at room temperature in 3% nonfat milk in TBS-T (TBS with 0.1% Tween) and incubated them with primary antibody at an appropriate dilution at 4 °C overnight in blocking buffer. We also diluted appropriate horseradish peroxidase–conjugated secondary antibodies in blocking buffer and incubated them with each membrane for 30 min at room temperature. We then washed filter membranes in TBS-T and visualized the immunolabeled proteins using ECL (Pierce).

Antibodies. We detected $p21^{cip1}$ using a mouse monoclonal primary antibody (clone SX118, BD Pharmingen) diluted 1:1,000; Mdm-2 using the mouse monoclonal antibody 2A10 at a 1:100 dilution; and β-actin with a mouse monoclonal primary antibody (Sigma) diluted 1:5,000. In all cases, secondary antibody to mouse conjugated with horseradish peroxidase was used at a 1:2,000 dilution. All antibodies were diluted in blocking buffer.

Real-time quantitative PCR analysis. We extracted RNA using a Qiagen RNase Easy kit in accordance with the manufacturer's instructions. We determined RNA concentration spectrophotometrically (NanoDrop) and confirmed the quality of RNA using a Bioanalyser (Agilent Technologies). We incubated total RNA with DNase I (DNA-free, Ambion) to remove contaminating DNA. We then inactivated the DNase and removed it in accordance with the manufacturer's specifications. We carried out control experiments with no reverse transcriptase on all samples to confirm that genomic DNA was no longer present. We reverse transcribed 300 ng of cleaned RNA in a 20-ml volume into cDNA using iScript (Bio-Rad) in accordance with the manufacturer's specifications. We carried out quantitative PCR analysis on an AB Prism 7900 sequence detection system (Applied Biosystems) using the fluorogenic 5′ nuclease assay[29] and calculated relative expression levels as described[30]. We designed assays (using Primer Express software v1.5, Applied Biosystems) with 6-FAM fluorophore at the 5′ end and the quencher BHQ1 at the 3′ end, and reactions were optimized to have >90% efficiency. We used primer and probe concentrations of 500 nM and 200 nM, respectively. We assayed cDNA equivalent to 3–5 ng of each RNA in triplicate by real-time PCR using QPCR master mix with final concentrations of 5.5 mM $MgCl_2$, 200 mM dNTPs and 0.5 units Hotstart Amplitaq Gold (AB) in 20-ml volumes in a 384-well plate. For normalization, we assayed cDNA equivalent to 3–5 ng of input RNA for ribosomal 18S RNA and β-glucuronidase. We chose β-glucuronidase and mouse 18S as controls because they were the least variable under our experimental conditions (data not shown). To detect transcriptional target messages of *Cdkn1a* and *Bbc3*, we used the probe and primer sets Mm00432448_m1 and Mm00519268_m1, respectively (Applied Biosystems).

Apoptosis, senescence and cell cycle assays. For 5-bromodeoxyuridine (BrdU)–propidium iodide flow cytometric analyses, we incubated cells in 50 mM BrdU for 5 h and then incubated them with fluorescein isothiocyanate–conjugated mouse monoclonal antibody to BrdU (Becton Dickinson) in

accordance with the company's protocol. For propidium iodide cell cycle profile analysis, we fixed cells overnight at 4 °C in 70% ethanol and stained them with propidium iodide at 50 mg ml^{-1}. We determined thymocyte apoptosis using flow cytometry by propidium iodide exclusion. All data points were normalized to unirradiated control thymocytes from the same mice. We carried out TUNEL staining of formalin-fixed, paraffin-embedded tissue sections with the ApopTag Apoptosis Detection Systems (Chemicon International). We used a peroxidase *in situ* apoptosis detection kit (Chemicon International) for histochemical identification of apoptosis in spleen and thymus and used a fluorescein direct *in situ* apoptosis detection kit (Chemicon International) for intestinal sections. We carried out staining for SA-β-galactosidase as described[31].

Induction of DNA damage in fibroblasts *in vitro* and mouse tissues *in vivo*. We treated MEFs with doxorubicin at a concentration of 0.5 ng ml^{-1} in the medium for 6 h. We collected cell lysates as described above. We treated mice with either 2.5 or 5 Gy of ionizing radiation from a Cs^{137} source.

ACKNOWLEDGMENTS

We thank L. Heath for help with interpretation of the pathology of the *Trp53*$^{KI/KI}$ tumors; P. Rodriquez-Viciana for the *H-ras V-12* retroviral vector; T. Littlewood for the p53minER vector; I. Rosewell for electroporation of ES cells; F. Rostker for assistance with animals; D. Ginzinger for Taqman analyses; A. Finch for assistance with histology and imaging; and F. McCormick, K. Shannon, D. Green, T. Tlsty, K. Vousden, R. Treisman, C. O'Shea, D. Iacovides and the members of the laboratory of G.I.E. for discussions, advice and criticism. This work was supported by grants from the US National Institutes of Health and by the University of California San Francisco Comprehensive Cancer Center Cell Cycle and Signaling Disregulation Program. D.M.-Z. was supported by grants from the Spanish Ministry of Science and Education. We dedicate our work to the memory of Stanley Korsmeyer.

COMPETING INTERESTS STATEMENT

The authors declare that they have no competing financial interests.

Received 29 November 2004; accepted 22 April 2005
Published online at http://www.nature.com/naturegenetics/

1. Sherr, C.J. Principles of tumor suppression. *Cell* **116**, 235–246 (2004).
2. Donehower, L.A. *et al.* Mice deficient for p53 are developmentally normal but susceptible to spontaneous tumours. *Nature* **356**, 215–221 (1992).
3. Vater, C., Bartle, L., Dionne, C., Littlewood, T. & Goldmacher, V. Induction of apoptosis by tamoxifen-activation of a p53-estrogen receptor fusion protein expressed in E1A and T24 H-ras transformed p53-/- mouse embryo fibroblasts. *Oncogene* **13**, 739–748 (1996).
4. Harvey, M., McArthur, M.J., Montgomery, C.A. Jr., Bradley, A. & Donehower, L.A. Genetic background alters the spectrum of tumors that develop in p53-deficient mice. *Faseb J.* **7**, 938–943 (1993).
5. Harvey, M. *et al.* Spontaneous and carcinogen-induced tumorigenesis in p53-deficient mice. *Nat. Genet.* **5**, 225–229 (1993).
6. Cui, Y.F. *et al.* Apoptosis in bone marrow cells of mice with different p53 genotypes after γ-rays irradiation *in vitro*. *J. Environ. Pathol. Toxicol. Oncol.* **14**, 159–163 (1995).
7. Botchkarev, V.A. *et al.* p53 is essential for chemotherapy-induced hair loss. *Cancer Res.* **60**, 5002–5006 (2000).
8. Fei, P., Bernhard, E.J. & El-Deiry, W.S. Tissue-specific induction of p53 targets *in vivo*. *Cancer Res.* **62**, 7316–7327 (2002).
9. Kemp, C.J., Sun, S. & Gurley, K.E. p53 induction and apoptosis in response to radio- and chemotherapy *in vivo* is tumor-type-dependent. *Cancer Res.* **61**, 327–332 (2001).
10. Komarova, E.A., Christov, K., Faerman, A.I. & Gudkov, A.V. Different impact of p53 and p21 on the radiation response of mouse tissues. *Oncogene* **19**, 3791–3798 (2000).
11. Potten, C.S., Merritt, A., Hickman, J., Hall, P. & Faranda, A. Characterization of radiation-induced apoptosis in the small intestine and its biological implications. *Int. J. Radiat. Biol.* **65**, 71–78 (1994).
12. Song, S. & Lambert, P.F. Different responses of epidermal and hair follicular cells to radiation correlate with distinct patterns of p53 and p21 induction. *Am. J. Pathol.* **155**, 1121–1127 (1999).
13. Lowe, S.W., Schmitt, E.M., Smith, S.W., Osborne, B.A. & Jacks, T. p53 is required for radiation-induced apoptosis in mouse thymocytes. *Nature* **362**, 847–849 (1993).
14. Attardi, L.D., de Vries, A. & Jacks, T. Activation of the p53-dependent G1 checkpoint response in mouse embryo fibroblasts depends on the specific DNA damage inducer. *Oncogene* **23**, 973–980 (2004).
15. Fei, P. & El-Deiry, W.S. p53 and radiation responses. *Oncogene* **22**, 5774–5783 (2003).
16. Midgley, C.A. *et al.* Coupling between γ irradiation, p53 induction and the apoptotic response depends upon cell type *in vivo*. *J. Cell Sci.* **108** (Pt 5), 1843–1848 (1995).
17. Ferbeyre, G. *et al.* Oncogenic ras and p53 cooperate to induce cellular senescence. *Mol. Cell. Biol.* **22**, 3497–3508 (2002).
18. Palmero, I., Pantoja, C. & Serrano, M. p19ARF links the tumour suppressor p53 to Ras. *Nature* **395**, 125–126 (1998).
19. Sherr, C.J. & DePinho, R.A. Cellular senescence: mitotic clock or culture shock? *Cell* **102**, 407–410 (2000).
20. Harvey, M. *et al.* *In vitro* growth characteristics of embryo fibroblasts isolated from p53-deficient mice. *Oncogene* **8**, 2457–2467 (1993).
21. Fukasawa, K., Wiener, F., Vande Woude, G.F. & Mai, S. Genomic instability and apoptosis are frequent in p53 deficient young mice. *Oncogene* **15**, 1295–1302 (1997).
22. Hanawalt, P.C., Ford, J.M. & Lloyd, D.R. Functional characterization of global genomic DNA repair and its implications for cancer. *Mutat. Res.* **544**, 107–114 (2003).
23. Adimoolam, S. & Ford, J.M. p53 and regulation of DNA damage recognition during nucleotide excision repair. *DNA Repair (Amst)* **2**, 947–954 (2003).
24. Hayflick, L. Living forever and dying in the attempt. *Exp. Gerontol.* **38**, 1231–1241 (2003).
25. Tarapore, P. & Fukasawa, K. Loss of p53 and centrosome hyperamplification. *Oncogene* **21**, 6234–6240 (2002).
26. Bienz, B., Zakut-Houri, R., Givol, D. & Oren, M. Analysis of the gene coding for the murine cellular tumour antigen p53. *EMBO J.* **3**, 2179–2183 (1984).
27. Littlewood, T.D., Hancock, D.C., Danielian, P.S., Parker, M.G. & Evan, G.I. A modified oestrogen receptor ligand-binding domain as an improved switch for the regulation of heterologous proteins. *Nucleic Acids Res.* **23**, 1686–1690 (1995).
28. White, I.N. Tamoxifen: is it safe? Comparison of activation and detoxication mechanisms in rodents and in humans. *Curr. Drug Metab.* **4**, 223–239 (2003).
29. Ginzinger, D.G. Gene quantification using real-time quantitative PCR: an emerging technology hits the mainstream. *Exp. Hematol.* **30**, 503–512 (2002).
30. Livak, K.J. & Schmittgen, T.D. Analysis of relative gene expression data using real-time quantitative PCR and the 2(-Delta Delta C(T)) Method. *Methods* **25**, 402–408 (2001).
31. Dimri, G.P. *et al.* A biomarker that identifies senescent human cells in culture and in aging skin *in vivo*. *Proc. Natl. Acad. Sci. USA* **92**, 9363–9367 (1995).

© 2005 Nature Publishing Group http://www.nature.com/naturegenetics